Fullerenes, Nanotubes and Carbon Nanostructures

ISSN: 1536-383X (Print) 1536-4046 (Online) Journal homepage: http://www.tandfonline.com/loi/lfnn20

Carbon nano-onion composites: Physicochemical characteristics and biological activity

Diana M. Bobrowska, Justyna Czyrko, Krzysztof Brzezinski, Luis Echegoyen & Marta E. Plonska-Brzezinska

To cite this article: Diana M. Bobrowska, Justyna Czyrko, Krzysztof Brzezinski, Luis Echegoyen & Marta E. Plonska-Brzezinska (2017) Carbon nano-onion composites: Physicochemical characteristics and biological activity, Fullerenes, Nanotubes and Carbon Nanostructures, 25:3, 185-192, DOI: 10.1080/1536383X.2016.1248758

To link to this article: http://dx.doi.org/10.1080/1536383X.2016.1248758

Accepted author version posted online: 27 Oct 2016.
Published online: 27 Oct 2016.

FULLERENES, NANOTUBES AND CARBON NANOSTRUCTURES
2017, VOL. 25, NO. 3, 185–192
http://dx.doi.org/10.1080/1536383X.2016.1248758

Taylor & Francis
Taylor & Francis Group

Carbon nano-onion composites: Physicochemical characteristics and biological activity

Diana M. Bobrowska[a], Justyna Czyrko[a], Krzysztof Brzezinski[a], Luis Echegoyen[b], and Marta E. Plonska-Brzezinska[a]

[a]Institute of Chemistry, University of Bialystok, Bialystok, Poland; [b]Department of Chemistry, University of Texas at El Paso, El Paso, Texas, USA

ABSTRACT

Carbon nano-onion/surfactant (CNO/surfactant) composites offer the possibility to easily produce the soluble nanostructures. That approach combines the hydrophilicity of surfactants with the robustness of carbon structures to produce composites with superior and unusual physicochemical properties. We used the following surfactants: hexadecyltrimethylammonium bromide (CTAB), sodium dodecyl sulfate (SDS), sodium dodecyl benzene sulfonate (SDBS), 4-(1,1,3,3-tetramethylbutyl)phenyl-polyethylene glycol (Triton X-100), and polyethylene glycol sorbitan monolaurate (Tween 20) to non-covalently modify CNO surfaces. The existence of stable CNO composites are clearly evidenced by direct transmission electron microscopy observations, which are also supported by thermogravimetric analyses. Dynamic light scattering and zeta potential confirmed their dispersion and stability. Additionally, the biological activity of well-dispersed CNO/surfactant composites against a strain of *Escherichia coli* was assayed. In vitro antimicrobial assays for the composites revealed that only the CNO/CTAB composite decreased cell viability. This activity could be assigned to the simple composite dissociation in water solutions, however antimicrobial properties of the composite are slightly better when compared with pure CTAB. This indicate some synergic effect with respect to the properties of the pure surfactant.

ARTICLE HISTORY
Received 2 September 2016
Accepted 10 October 2016

KEYWORDS
Antibacterial activity; Carbon nano-onions; Composites; Nanostructures; Antibacterial activity

1. Introduction

Material chemistry mainly involves the synthesis of new materials or modification of exciting ones to obtain properties for specific applications (1,2). A lot of attention has been devoted to nanometric scale structures. Carbon nanoparticles have been quite commonly used in many applications, mainly due to their large surface areas, high thermal stabilities, unusual electronic properties and broad absorption spectra (3,4). Their electronic properties determine their applications as biosensors, in photovoltaics systems (5–9), and electronics (10–15). There are still limitations in the preparation of well-dispersed carbon nanomaterials in aqueous solutions. Our research to date indicates that carbon nano-onions (CNOs) seem to be promising materials since they exhibit high reactivity due to their relatively small sizes (16). The most common method for the preparation of CNOs is based on the thermal annealing of ultradispersed nanodiamonds (NDs) of a few nanometers diameter under a He atmosphere and temperatures in the range between 1500 and 1800°C (17). Using NDs with a diameter of 5 nm led to formation of spherical CNOs with a diameter in the range between 5 and 6 nm, that correspond to the nanostructures with 6–8 concentric fullerene layers and a distance between them of 0.334 nm (18).

Non-modified carbon nanostructures (CNs) have somewhat limited dispersibility in many solvents thus hindering their applicability. Covalent functionalization of CNs changes sp^2 to sp^3 carbon a hybridization and alters their electronic properties (19). The noncovalent functionalization of carbon structures with polymers or surfactants dispersing agents is an effective approach to retain the intrinsic properties of the CN structures (20–23).

Surfactants are a unique class of chemical compounds with interesting chemical and physical properties, which have the ability to alter the surface and interfacial properties of different nanostructures (24). Surfactants form structured molecular assemblies in solution and their structures and properties depend on the concentration, temperature, and other condition (25). These structures can solubilize various molecular species to form host–guest systems, but they can also be applied as matrices for the incorporation of various organic and inorganic materials (26,27). These can lead to an increase of the wettability of the nanostructures and to stabilization of their dispersions (28). Their 'surface-active' properties make them useful as industrial cleaners, in personal care products, cosmetics (29), pharmaceuticals, and in biochemical research involving electrophoresis (30,31). It has also been shown that some surfactants are sensitive to bacterial biodegradation, thus they are used in transepidermal, nasal, and ocular drug delivery systems (32,33).

A wide variety of water-soluble additives has been successfully used for the modification of CNOs (34,35). In this work, we selected commonly used surfactants with cationic, anionic and non-ionic character, such as hexadecyltrimethylammonium

CONTACT Marta E. Plonska-Brzezinska mplonska@uwb.edu.pl University of Bialystok, Ciolkowskiego 1K, 15-245 Bialystok, Poland.

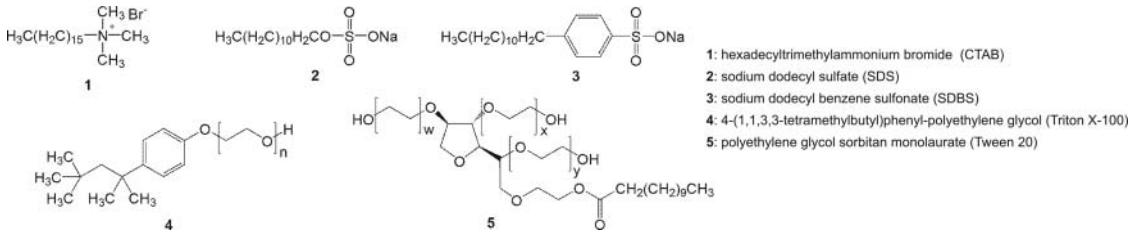

Scheme 1. Surfactants used for the modification of CNOs.

bromide (CTAB, 1), sodium dodecyl sulfate (SDS, 2), sodium dodecyl benzene sulfonate (SDBS, 3), 4-(1,1,3,3-tetramethylbutyl) phenyl-polyethylene glycol (Triton X-100, 4), and polyethylene glycol sorbitan monolaurate (Tween 20, 5) (Scheme 1). In this study, several techniques were used to probe the association between surfactants and carbon nano-onions. We report the stabilization of CNOs in aqueous media in the presence of the different surfactants. The composites were also tested as antibacterial agents. The results demonstrate that only the CNO/CTAB composite reveals significant antibacterial activity.

2. Materials

All chemicals and solvents used were commercially available and were used without additional purification: sodium dodecyl sulfate (≥99.0%, Sigma Aldrich) (SDS), sodium dodecylbenzenesulfonate (technical grade, Sigma-Aldrich) (SDBS), hexadecyltrimethylammonium bromide (≥98.0%, Sigma-Aldrich) (CTAB), 4-(1,1,3,-tetramethylbutyl)phenyl-polyethylene glycol (laboratory grade, Sigma-Aldrich) (Triton X-100), Tween 20 (Alfa Aesar GmbH&Co), ethyl alcohol absolute (99.8%, POCH), ATPlite kit (PerkinElmer), multi-well filter plate (Pall Corporation), 96-well microplate- CulturPlate (Perkin Elmer), nanodiamond powder (Carbodeon μDiamond® Molto) with a crystal size between 4 and 6 nm, and ND content ≥97 wt.%.

2.1. Synthesis of carbon nano-onions

Annealing of ultradispersed nanodiamonds was performed at 1650°C under a 1.1 mPa He atmosphere with a heating ramp of 20°C min^{-1} in an Astro carbonization furnace (17). The final temperature was maintained for 1 hour, then the material was slowly cooled to room temperature over a period of 1 hour. Next, the CNOs were annealed in air at 400°C to remove any amorphous carbon (36).

2.2. Synthesis of CNO/surfactant composites

Composites of CNOs and surfactants was prepared as follows: five different concentrations of surfactants – 100, 10, 1, 0.1 and 0.01 mg mL^{-1} were added to 1 mg of crude CNOs. CNOs with each surfactants were suspended via pulse probe sonication by 30 min with 35 kHz frequency. Subsequently, the composite materials were centrifuged and the excess of surfactant solutions was removed. CNOs with adsorbed surfactant on their surface of five different initial concentrations were obtained.

3. Methods

Transmission Electron Microscopic images were recorded using the FEI Tecnai^{TM} G2 20 X-TWIN instrument. The TEM point resolution was 0.25 nm, the TEM line resolution was 0.144 nm, the maximum diffraction angle was ±12°, and the working distance was 10 mm. The accelerating voltage of the electron beam was 200 keV (37).

Particle size and ζ-potential were determined using Dynamic Light Scattering (DLS) with the NanoPlus DLS Nano Particle Size and Zeta Potential Analyzer. Particle size studies were done using 1 cm quartz cells, however for the zeta potential measurements a flow cell was used. The NanoPlus DLS measures the particle sizes of samples suspended in liquids in the range of 0.1 nm to 12.30 μm. The ζ-potential of sample suspensions were measured in the −200 mV to +200 mV range. The ζ-potential values determined using the Smoluchowski equation are the average of 10 repeated measurements.

Differential-thermogravimetric (TGA-DTG) analyses were performed by a Thermal Analyzer TGA/DSC 1 (METTLER TOLEDO) with a heating rate of 10°C min^{-1} under an oxygen atmosphere with a flow rate of 10 mL min^{-1}. The measurements were conducted in alumina crucibles with lids in the temperature range from 50 to 1000°C.

3.1. Antibacterial activity assay

Two milligrams of each composite or unmodified CNOs was suspended in 1 mL of *Luria-Bertani Broth* (LB) medium containing 34 μg·mL^{-1} chloramphenicol. The suspension (from 10 to 100 μL) was transferred into 96 deep-well plates and filled with the medium up to 100 μL. Separately, 10 mL of LB medium supplemented with the antibiotics was inoculated with BL21-CodonPlus(DE3)®-RIPL strain of *Escherichia coli* and grown overnight at 28°C. The overnight culture was used for inoculation of 50 mL of the fresh medium and grown to an OD_{600nm} of 0.9. Next, the culture was diluted with the medium in the ratio 1:1 and transferred (100 μL) to deep-well plates with CNO suspensions. The cultures were incubated in a shaker at 28°C for 2 hours. Cell viability was assessed by the luminescence ATP detection assay system (ATPlite). The assay was performed according to the procedure described by the manufacturer with some deviations. Briefly, after the culture incubation, 100 μL of cell lysis solution was added to each plate cell and shaken for 5 min. To remove suspended CNOs, the lysate was filtered with 0.2 μm multi-well filter plate and subsequently centrifuged. Next, 100 μL of the supernatant was transferred to white 96-well microplate and 50 μL of substrate solution was added to

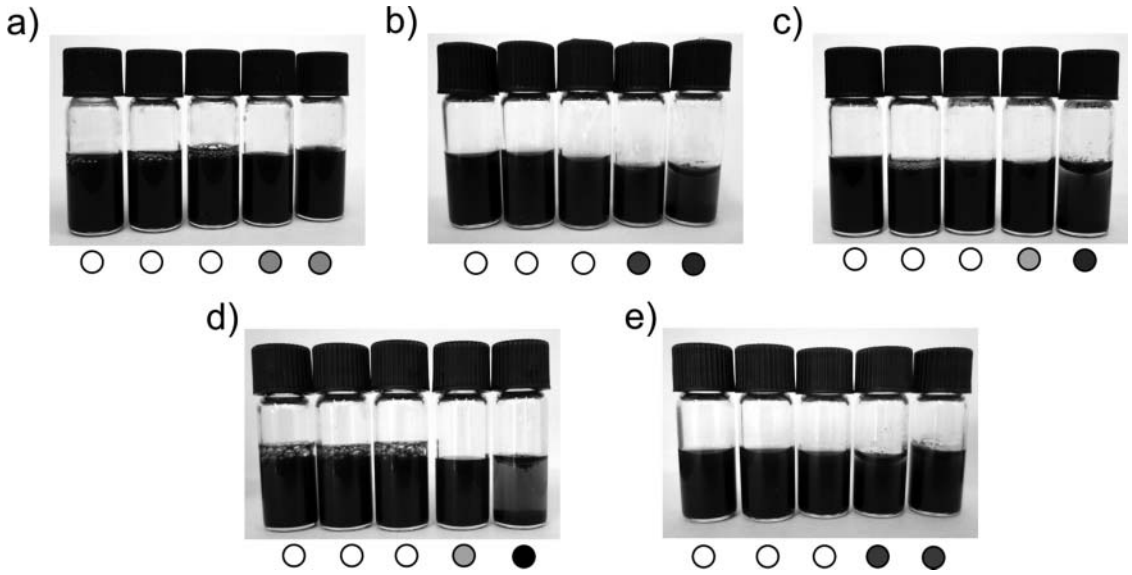

Scheme 2. Photographs of the CNO dispersions after standing for 1 day with different concentrations of: (1) CTAB, (2) SDBS, (3) SDS, (4) Triton X-100, and (5) Tween 20. Different mass ratios of surfactants to CNOs (from left to right in each subsection): 100:1, 10:1, 1:1, 1:10, and 1:100 mg mL^{-1}. Shaded circles represent the presence of visible precipitates.

each well and shaken for 5 min. Luminescence was measured at 25°C using a microplate reader (Tecan Infinite M200 Pro). Bacteria culture was used as a negative control. Also, the reference tests were performed with the pure surfactants. For each tested composite concentration and adequate reference, we used the same surfactant concentration. The surfactant content in composites was established on the basis of TGA experiments. All measurements were performed in triplicates.

4. Results

4.1. Preparation and characterization of CNO/surfactant composites

Water solubilization of nanoparticles is an essential condition for their biological application. Due to the low dispersion ability of CNOs in aqueous solutions, attaching hydrophilic chains can lead to water-soluble derivatives. To investigate the optimal

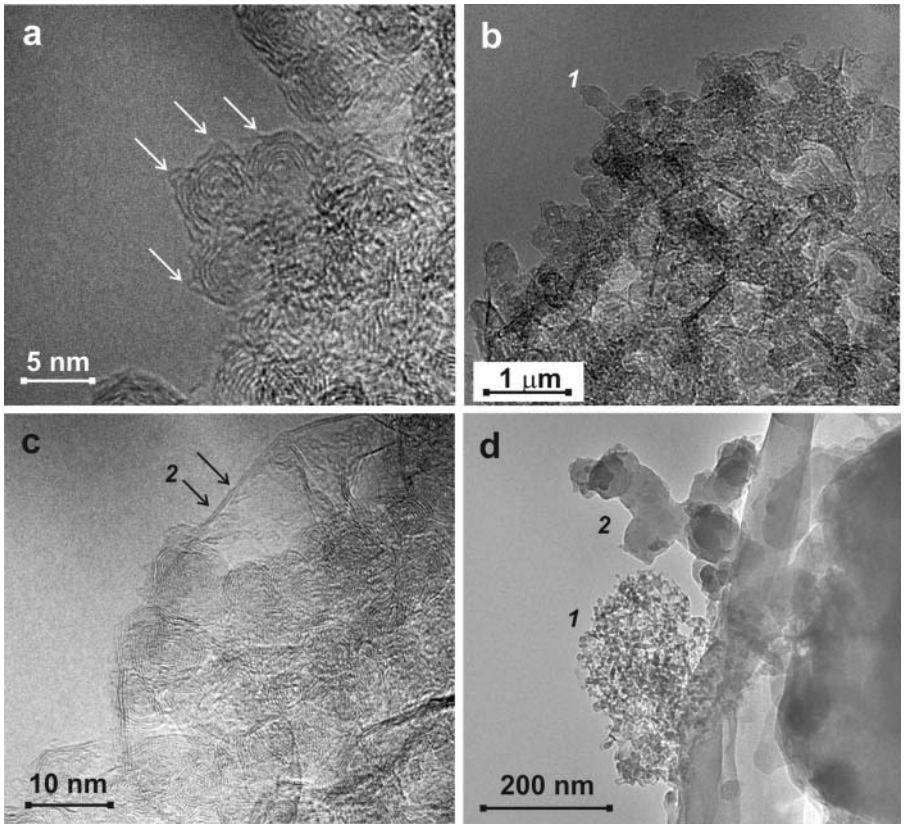

Figure 1. TEM images of the CNO/CTAB composites with the concentrations of CTAB: (a,b) 0.01; (c) 1; and (d) 100 mg mL^{-1} in starting material.

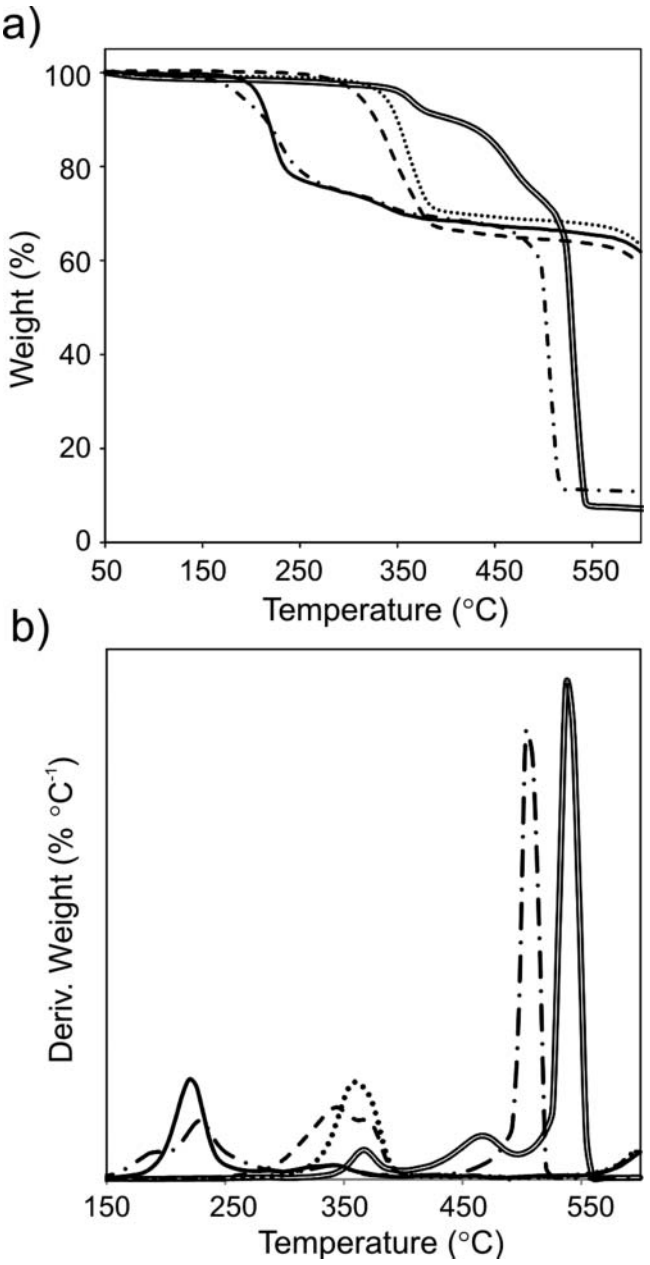

Figure 2. (a) TGA and (b) DTG curves of CNOs/SDS (.—.—), CNOs/SDBS (═══), CNOs/CTAB (——), CNOs/Tween 20 (···), and CNOs/Triton X (— — —). Concentrations of surfactants were 1:1 (mass ratio of both components) in the starting material.

concentration of surfactants for CNO composite formation, different concentrations of surfactants (100, 10, 1, 0.1, and 0.01 mg mL^{-1} in the starting material) were added to 1 mg mL^{-1} of crude CNOs. CNOs were suspended via probe sonication. The different mass ratios led to stable dispersions of the carbon material (see Scheme 2).

The interactions between the CNOs and the surfactants resulted in the formation of large aggregates. The stability of the water-dispersed CNOs also depended on the surfactant concentrations (Scheme 2). The most stable CNO/surfactant composites are formed at low surfactant concentrations in the range between 1 and 0.01 mg mL^{-1}. Under those conditions, the systems are very homogenous suggesting a complete dispersion of the carbon nanoparticles. In contrast, some composites contain fine dust and inhomogencittes (see Scheme 2).

The Transmission Electron Microscopy (TEM) images (Figure 1) of the CNO composites showed the presence of both components: surfactant (structure 2) and carbon-based (structure 1) in the composite matrices. TEM clearly revealed surfactant wrapping of CNOs and showed a significant increase of the amount of surfactant in the composites, compare Figure 1a, c, and d. As shown in Figure 1, increasing the concentration of the surfactants resulted in the formation of island-like structures of the composites (Figure 1d, structures 1 and 2). Homogenous core-shell nanostructures were obtained for low concentration of surfactant in the composite, about 0.01 mg mL^{-1} of surfactant in the starting material (Figure 1a and b).

Differential-thermogravimetric analyses (TGA-DTG) of the CNO composites with the different surfactants were performed to detect the surfactants and to probe the thermal stability of the composites under an air atmosphere at 10°C min^{-1}. The thermal behavior of the CNO composites is important to evaluate the applicability of these materials. The results are presented in Figure 2. When the samples were heated under air, the surfactants thermally decomposed from 160 to 470°C. The surfactant mass losses are presented in Figure 2 and Table 1. All composites contained ca. 30–35 wt % of the surfactant units wrapped on the CNO surface for the composites 1:1 (mass ratio of both components in the starting materials). The combustion of the CNOs started at temperatures higher than ca. 470°C for the composites containing SDS and SDBS. The other composites showed higher thermal stabilities with inflection temperatures for the carbon materials around 620°C.

The modification of the CNO surface with surfactants was also confirmed by Dynamic Light Scattering (DLS) and zeta (ζ) potential measurements, which are presented in Figure 3 and Table 2. We performed DLS measurements to determine the average hydrodynamic diameters and size distributions of the CNO/surfactant structures in aqueous solutions. The

Table 1. The TGA-DTG parameters of the CNO composites.

Sample	Onset temperature (°C)	Inflection temperature (°C)	End temperature (°C)	Total weight loss of composite (%)
CNOs/SDS	160	345,[a] 370,[a] 503[b]	410	32
CNOs/SDBS	330	367,[a] 463,[a] 527[b]	540	35
CNOs/CTAB	180	220,[a] 635[b]	450	35
CNOs/Tween 20	295	362,[a] 620[b]	400	30
CNOs/Triton X	260	230,[a] 620[b]	395	35

[a]The temperature for surfactants.
[b]The temperature for CNOs. Concentrations of surfactants were 1:1 (mass ratio of both components) in the starting material.

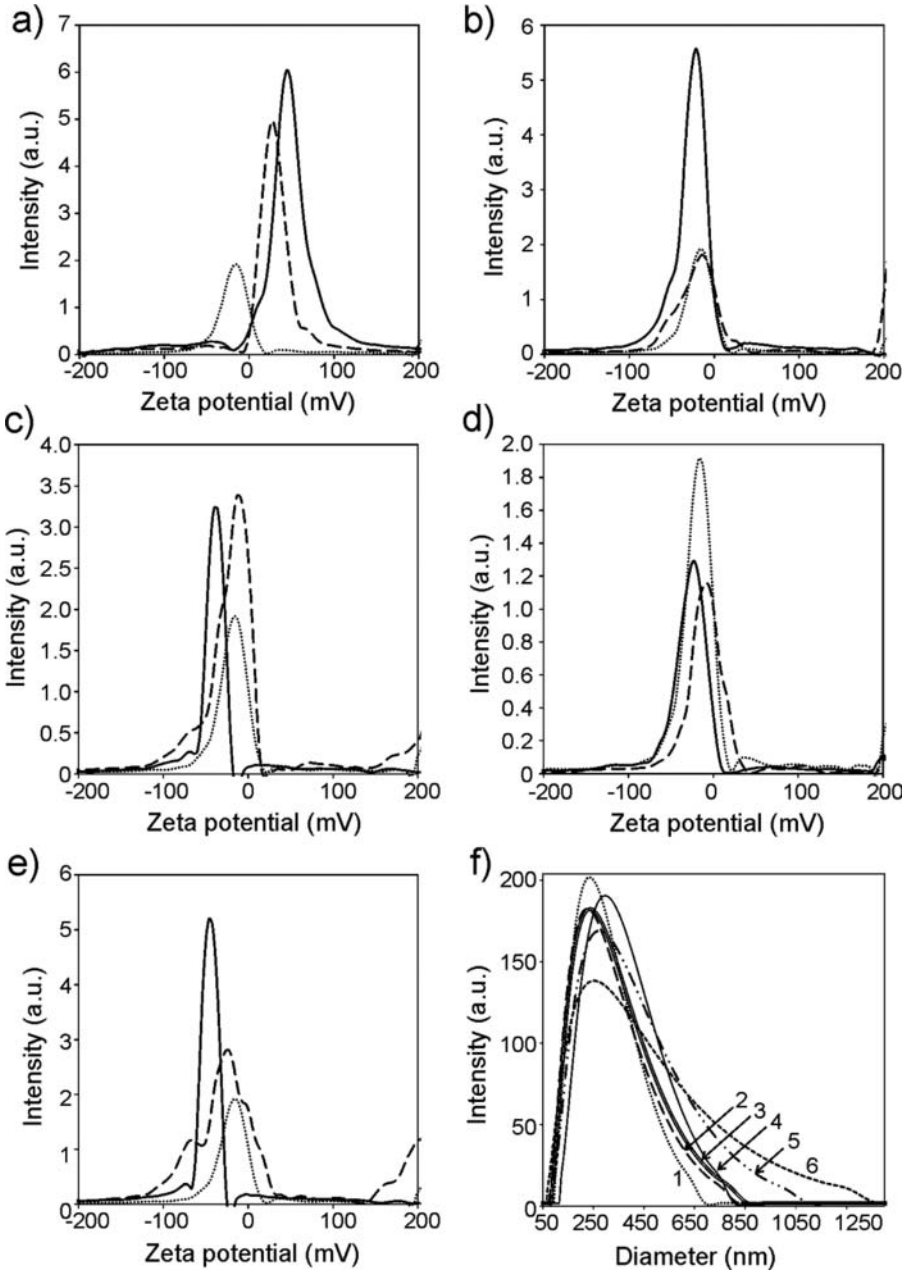

Figure 3. Zeta potential of CNOs/surfactants (——), and their references: CNOs (·····) and pristine surfactant (– – –): (a) CNOs/CTAB, (b) CNOs/Triton-X, (c) CNOs/SDS, (d) CNOs/Tween, (e) CNOs/SDBS. (f) Diameter of CNOs with surfactants: (1) CNOs/SDBS (·····), (2) CNOs/Triton-X (– – –), (3) CNOs/CTAB (═══), (4) CNOs (——), (5) CNOs/SDS (–..–), and (6) CNOs/Tween (- - - -). The relative CNO/surfactant ratio for the composites was 0.01 mg mL^{-1}.

Stokes-Einstein equation (38):

$$D_S = \frac{kT}{f} = \frac{kT}{6\pi\eta R_H} \quad (1)$$

allows the determination of the hydrodynamic radius of the scattering particle (R_H), when the temperature (T), solvent viscosity (η), and self diffusion coefficients are measured for very dilute samples using dynamic light scattering. As is well known, the aggregation behaviour of monomeric surfactants in solution is controlled by the inter-molecular interaction of the monomeric surfactants and the inter-molecular interaction of the surfactants with the carbon nanoparticles and their interactions with solvents (39–41,42). In general, the sizes of the CNO/surfactant composites in solution differ from these of the pristine CNO nanoparticles, the latter forming larger aggregates (Table 2), due to van der Waals interactions between the carbon nanostructures. As expected, the average number of adsorbed aggregates increases with the addition of surfactants and attains an equilibrium value. The interaction between CNOs and surfactants led to the formation of spherical aggregates with maximum sizes ranging from 230 nm to 330 nm (Figure 3f and Table 2).

Zeta potential measurements were performed for the CNO composites to characterize the surface charge on the nanoparticles and their stability in solution. The stepwise adsorption of surfactants was followed by checking the surface charge of the aggregates upon the addition of surfactants to a CNO dispersion. The measurements of the zeta potential of the surfactant-treated

Table 2. Dynamic light scattering and zeta potential results in aqueous solution for CNO/surfactant composites.

Materials	Hydrodynamic diameter (D_H) (nm) with standard deviation[a]	Zeta potential (mV) with standard deviation[b]
CNOs	488 ± 24	−17 ± 1
CTAB	—	31 ± 3
CNOs/CTAB	259 ± 3	45 ± 1
SDS	—	−17 ± 3
CNOs/SDS	323 ± 34	−39 ± 1
SDBS	—	−30 ± 7
CNOs/SDBS	271 ± 9	−45 ± 1
Triton	—	−19 ± 1
CNOs/Triton	240 ± 4	−34 ± 1
Tween	—	−9 ± 1
CNOs/Tween	234 ± 5	−35 ± 1

Concentrations of surfactants were 0.01 mg mL^{-1}.
[a]Standard deviation was calculated based on 15 measurements.
[b]Standard deviation was calculated based on 10 measurements.

CNOs at pH 7.4 reflected the alteration of the surface charge distribution, as shown in Figure 3 and Table 2. The surface charge increased from the lower to higher value of ζ-potential, confirming the stepwise coating of CNOs with surfactants (Figure 3a–f, Table 2). As indicated, an increase of the surface charge was induced upon the adsorption of surfactants. The ζ-potential gives also important information on the stability of the aggregate suspensions. Particles with ζ-potential values between +30 mV and −30 mV are considered to be stable because of the strong repulsion forces that prevent their aggregation (43). Values higher than ±30 mV were observed for all CNO composites. The high zeta potentials of such dispersions confirm that the CNOs are well-stabilized by the surfactants, thus inhibiting aggregation. The ζ-potential values, together with the sizes, confirm the presence of stable CNO/surfactant composites.

4.2. Antibacterial activity of the CNO/surfactant composites

Antibacterial activity assays performed with *Escherichia coli* cultures after 2 hours treatment with CNOs/surfactants and with non-modified CNOs demonstrated that only the CNO/CTAB composite showed a dose-dependent response (Figure 4). The composite significantly decreased cell viability (~40%) in response to 200 μg mL^{-1} and caused a further ~70% loss in viability in response to 300 μg mL^{-1} of the composite. An antibacterial response is also observed for the pure CTAB, however the composite reveals stronger antibacterial activity in lower concentration range. This indicate some synergic effect of the composite with respect to the pure surfactant. Detergents can affect a bacterial viability by disrupting cell membranes which lead to cell lysis. This process requires the interaction of dissolved surfactants with the cell membrane. We suggest that the antibacterial activity of the CNO/CTAB composite is at least partially the result of its dissociation in solution, however this phenomenom cannot explain the synergy of CNO and CTAB in antimicrobial tests. On the other hand, non-modified CNOs and composites containing SDS, Triton X100 and SDBS have no or little effect on the bacteria cell viability when compared to the negative control and pure detergents. This indicates the surfactant activity is inhibited when adsorbed on the CNO surface. The lack of antimicrobial properties for the other composites is probably the result of higher stabilities in aqueous solutions. Results for CNO/Tween 20 composite, as well as the pure surfactant indicate that their concentration are too low to observed significant decrease of viability of bacterial cells.

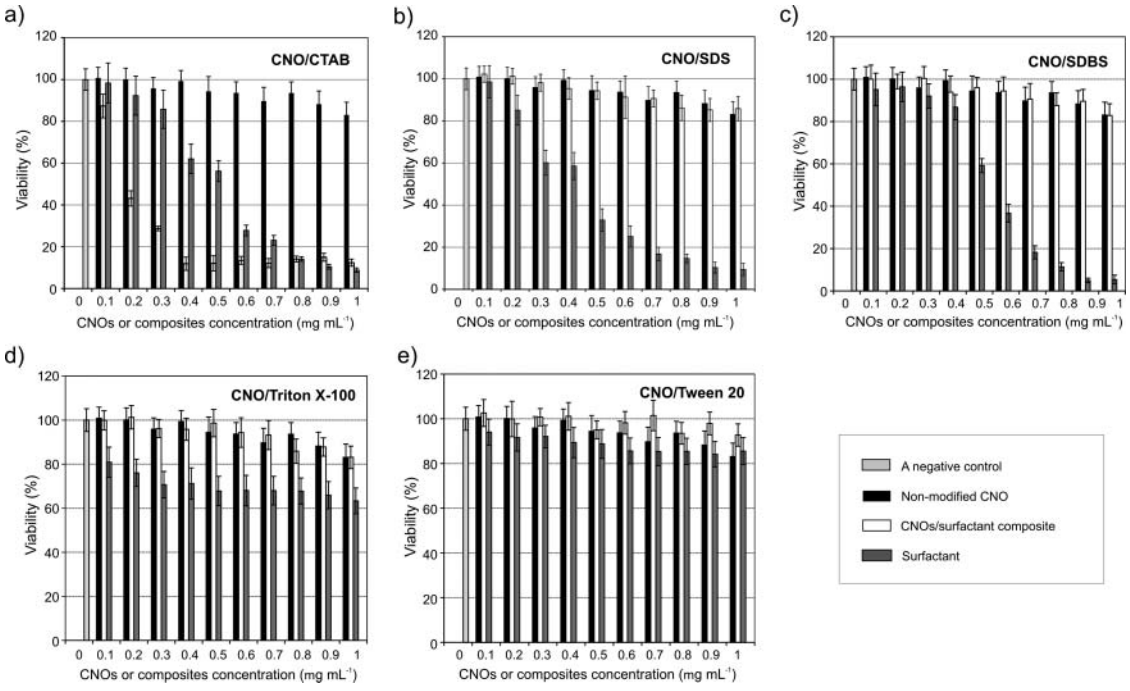

Figure 4. Viability of *Escherichia coli* cells after exposition to ten concentrations of the CNO/surfactant composites and non-modified CNOs, as well as ten concentrations of surfactants corresponding to the surfactant contents in the composites used in antimicrobial tests, established with TGA experiments. For clarity only concentrations of CNO and composites are shown. Viability was tested using the ATPLite assay and results are expressed as a percentage of the negative control (bacteria culture without any additives). Data are expressed as mean ± standard error.

5. Conclusions

Much effort has been devoted to the development of different techniques for the dispersion of carbon nanostructures in solution, with one promising method involving the use of aqueous solutions of surfactants that show long-term stabilities. We used different surfactants to prepare CNO composites with well-defined properties. The existence of stable CNO composites are clearly evidenced by direct TEM observations, which are also supported by measurements of micellar sizes by dynamic light scattering and thermogravimetric analyses. Dynamic light scattering and zeta potential confirmed their high dispersion and stability. *In vitro* antimicrobial assays for the composites revealed that only the CNO/CTAB composite decreased cell viability. This activity is at least the result of composite dissociation in water solutions, however some synergic effect is also observed for the composite.

Acknowledgments

We gratefully acknowledge the financial support of the National Science Centre, Poland (grant: #2011/01/B/ST5/06051) to M.E.P.-B. L.E. thanks the Robert A. Welch Foundation for an endowed chair, grant #AH-0033 and the US NSF, grants: DMR-1205302 and CHE-1408865. TEM and DLS were funded by the European Funds for Regional Development as part of the Operational Programme Development of Eastern Poland 2007–2013 (projects: POPW.01.03.00-20-034/09 and POPW.01.03.00-20-004/11).

References

1. Coudert, F-X. (2015) Responsive Metal–Organic frameworks and framework materials: Under pressure, taking the heat, in the spotlight, with friends. *Chem Mater*, 27(6): 1905–1916.
2. Kim, B. H., Hackett, M. J., Park, J., and Hyeon, T. (2014) Synthesis, characterization, and application of ultrasmall nanoparticles. *Chem. Mater.*, 26(1): 59–71.
3. Wang, S., Gao, R., Zhou, F., and Selke, M. (2004) Nanomaterials and singlet oxygen photosensitizers: potential applications in photodynamic therapy. *J. Mater. Chem.*, 14(4): 487.
4. Xie, Q., Perez-Cordero, E., and Echegoyen, L. (1992) Electrochemical detection of C606- and C706-: Enhanced stability of fullerides in solution. *J. Am. Chem. Soc.*, 114(10): 3978–3980.
5. Sariciftci, N. S., Smilowitz, L., Heeger, A. J., and Wudl, F. (1992) Photoinduced electron transfer from a conducting polymer to buckminsterfullerene. *Science*, 258(5087): 1474–1476.
6. Lenes, M., Shelton, S. W., Sieval, A. B., Kronholm, D. F., Hummelen, J. C. (Kees)., and Blom, P. W. M. (2009) Electron trapping in higher adduct fullerene-based solar cells. *Adv. Funct. Mater.*, 19(18): 3002–3007.
7. Sariciftci, N. S., Braun, D., Zhang, C., Srdanov, V. I., Heeger, A. J., Stucky, G., et al. (1993) Semiconducting polymer-buckminsterfullerene heterojunctions: Diodes, photodiodes, and photovoltaic cells. *Appl. Phys. Lett.*, 62(6): 585.
8. Hummelen, J. C., Knight, B. W., LePeq, F., Wudl, F., Yao, J., and Wilkins, C. L. (1995) Preparation and characterization of fulleroid and methanofullerene derivatives. *J. Org. Chem.*, 60(3): 532–538.
9. Yu, G., Gao, J., Hummelen, J. C., Wudl, F., and Heeger, A. J. (1995) Polymer photovoltaic cells: Enhanced efficiencies via a network of internal donor-acceptor heterojunctions. *Science*, 270(5243): 1789–1791.
10. Martin, N. (2006) New challenges in fullerene chemistry. *Chem. Commun.*, 20: 2093.
11. Rao, C. N. R., Sood, A. K., Subrahmanyam, K. S., and Govindaraj, A. (2009) Graphene: The new Two-dimensional nanomaterial. *Angew. Chem. Int. Ed.*, 48(42): 7752–7777.
12. Novoselov, K. S. (2004) Electric field effect in atomically thin carbon films. *Science*, 306(5696): 666–669.
13. Novoselov, K. S., Geim, A. K., Morozov, S. V., Jiang, D., Katsnelson, M. I., Grigorieva, I. V., et al. (2005) Two-dimensional gas of massless Dirac fermions in graphene. *Nature*, 438(7065): 197–200.
14. Chen, R. J., Choi, H. C., Bangsaruntip, S., Yenilmez, E., Tang, X., Wang, Q., et al. (2004) An investigation of the mechanisms of electronic sensing of protein adsorption on carbon nanotube devices. *J. Am. Chem. Soc.*, 126(5): 1563–1568.
15. Ishikawa, F. N., Curreli, M., Olson, C. A., Liao, H-I., Sun, R., Robertsm, R. W., et al. (2010) Importance of controlling nanotube density for highly sensitive and reliable biosensors functional in physiological conditions. *ACS Nano.*, 4(11): 6914–6922.
16. Rettenbacher, A. S., Elliott, B., Hudson, J. S., Amirkhanian, A., and Echegoyen, L. (2006) Preparation and functionalization of multilayer fullerenes (Carbon Nano-Onions). *Chem - Eur. J.*, 12 (2): 376–387.
17. Kuznetsov, V. L., Chuvilin, A. L., Butenko, Y. V., Mal'kov, I. Y., and Titov, V. M. (1994) Onion-like carbon from ultra-disperse diamond. *Chem. Phys. Lett.*, 222(4): 343–348.
18. Bacon, R. (1960) Growth, structure, and properties of graphite whiskers. *J. appl. Phys.*, 31(2): 283.
19. Kötz, R. and Carlen, M. (2000) Principles and applications of electrochemical capacitors. *Electrochim. Acta.*, 45(15–16): 2483–2498.
20. Plonska-Brzezinska, M. E., Mazurczyk, J., Palys, B., Breczko, J., Lapinski, A., Dubis, A. T., et al. (2012) Preparation and characterization of composites that contain small carbon Nano-onions and conducting polyaniline. *Chem. Eur. J.*, 18(9): 2600–2608.
21. Breczko, J., Winkler, K., Plonska-Brzezinska, M. E., Villalta-Cerdas, A., and Echegoyen, L. (2010) Electrochemical properties of composites containing small carbon nano-onions and solid polyelectrolytes. *J. Mater. Chem.*, 20(36): 7761.
22. Kovalenko, I., Bucknall, D. G., and Yushin, G. (2010) Detonation nanodiamond and Onion-like-carbon-embedded polyaniline for supercapacitors. *Adv. Funct. Mater.*, 20(22): 3979–3986.
23. Rettenbacher, A. S., Perpall, M. W., Echegoyen, L., Hudson, J., and Smith, D. W. (2007) Radical addition of a conjugated polymer to multilayer fullerenes (Carbon Nano-onions). *Chem. Mater.*, 19(6): 1411–1417.
24. Schramm, L. L., Stasiuk, E. N., and Marangoni, D. G. (2003) Surfactants and their applications. *Annu. Rep. Sect. C. Phys. Chem.*, 99: 3.
25. Ruiz-Hitzky, E., Aranda, P., Darder, M., and Ogawa, M. (2011) Hybrid and biohybrid silicate based materials: molecular vs. block-assembling bottom–up processes. *Chem. Soc. Rev.*, 40(2): 801–828.
26. Amjad, Z. (2011) Impact of surfactants on the efficacy of iron oxide dispersants. *Tenside Surfactants Deterg*, 48(3): 190–196.
27. Cavalcante Hissa, D., Arruda Bezerra, G., Birner-Gruenberger, R., Paulino Silva, L., Usónm, I., Gruber, K., et al. (2014) Unique crystal structure of a novel surfactant protein from the foam nest of the frog leptodactylus vastus. *Chem. Bio. Chem.*, 15(3): 393–398.
28. Dung Dang, T. M., Tuyet Le, T. T., Fribourg-Blanc, E., and Chien Dang, M. (2011) The influence of solvents and surfactants on the preparation of copper nanoparticles by a chemical reduction method. *Adv. Nat. Sci. Nanosci Nanotechnol*, 2(2): 25004.
29. Singer, M. M. and Tjeerdema, R. S. (1933) Fate and effects of the surfactant sodium dodecyl sulfate. *Rev. Environ. Contam. Toxicol*, 133: 95–149.
30. Towns, J. K. and Regnier, F. E. (1991) Capillary electrophoretic separations of proteins using nonionic surfactant coatings. *Anal. Chem.*, 63(11): 1126–1132.
31. Karlsson, R., Karlsson, A., Ewing, A., Dommersnes, P., Joanny, J-F., Jesorka, A., et al. (2006) Chemical analysis in nanoscale surfactant networks. *Anal. Chem.*, 78(17): 5960–5968.
32. Lima, T. M. S., Procópio, L. C., Brandão, F. D., Carvalho, A. M. X., Tótola, M. R., and Borges, A. C. (2011) Biodegradability of bacterial surfactants. *Biodegradation*, 22(3): 585–592.
33. Marchesi, J. R., Russell, N. J., White, G. F., and House, W. A. (1991) Effects of surfactant adsorption and biodegradability on the distribution of bacteria between sediments and water in a freshwater microcosm. *Appl. Environ. Microbiol*, 57(9): 2507–2513.

34. Zhou, L., Gao, C., Zhu, D., Xu, W., Chen, F. F., Palkar, A., et al. (2009) Facile functionalization of multilayer fullerenes (carbon nano-onions) by Nitrene chemistry and "Grafting from" strategy. *Chem. Eur. J.*, 15 (6): 1389–1396.
35. Shenderova, O., Jones, C., Borjanovic, V., Hens, S., Cunningham, G., Moseenkov, S., et al. (2008) Detonation nanodiamond and onion-like carbon: applications in composites. *Phys. Status Solidi A*, 205(9): 2245–2251.
36. Plonska-Brzezinska, M. E., Brus, D. M., Molina-Ontoria, A., and Echegoyen, L. (2013) Synthesis of carbon nano-onion and nickel hydroxide/oxide composites as supercapacitor electrodes. *RSC Adv.*, 3 (48): 25891.
37. Mykhailiv, O., Lapinski, A., Molina-Ontoria, A., Regulska, E., Echegoyen, L., Dubis, A. T., et al. (2015) Influence of the synthetic conditions on the structural and electrochemical properties of carbon nano-onions. *Chem. Phys. Chem.*, 16(10): 2182–2191.
38. Edward, J. T. (1970) Molecular volumes and the Stokes-Einstein equation. *J. Chem. Educ.*, 47(4): 261.
39. Mondal, S., Das, T., Ghosh, P., Maity, A., Mallick, A., and Purkayastha, P. (2015) Surfactant chain length controls photoinduced electron transfer in surfactant bilayer protected carbon nanoparticles. *Mater. Lett.*, 141: 252–254.
40. Wang, M., Wu, C., Tang, Y., Fan, Y., Han, Y., and Wang, Y. (2014) Interactions of cationic trimeric, gemini and monomeric surfactants with trianionic curcumin in aqueous solution. *Soft. Matter*, 10(19): 3432.
41. Choe, S., Chang, R., Jeon, J., and Violi, A. (2008) Molecular dynamics simulation study of a pulmonary surfactant film interacting with a carbonaceous nanoparticle. *Biophys J.*, 95(9): 4102–4114.
42. Han, Y. and Wang, Y. (2011) Aggregation behavior of gemini surfactants and their interaction with macromolecules in aqueous solution. *Phys. Chem. Chem. Phys.*, 13(6): 1939.
43. Eldridge, J. A., Willmott, G. R., Anderson, W., and Vogel, R. (2014) Nanoparticle ζ-potential measurements using tunable resistive pulse sensing with variable pressure. *J. Colloid Interface Sci.*, 429: 45–52.